UPPSALA
UNIVERSITET

Digital Comprehensive Summaries of Uppsala Dissertations from the Faculty of Science and Technology 1795

Adaptation of wave power plants to regions with high tides

MOHD NASIR AYOB

ACTA
UNIVERSITATIS
UPSALIENSIS
UPPSALA
2019

ISSN 1651-6214
ISBN 978-91-513-0627-8
urn:nbn:se:uu:diva-381169

Dissertation presented at Uppsala University to be publicly examined in Room 2001, Ångströmlaboratoriet, Lägerhyddsvägen 1, Uppsala, Wednesday, 22 May 2019 at 09:00 for the degree of Doctor of Philosophy. The examination will be conducted in English. Faculty examiner: Professor Ian Masters (Swansea University).

Abstract
Ayob, M. N. 2019. Adaptation of wave power plants to regions with high tides. *Digital Comprehensive Summaries of Uppsala Dissertations from the Faculty of Science and Technology* 1795. 53 pp. Uppsala: Acta Universitatis Upsaliensis. ISBN 978-91-513-0627-8.

The wave energy converter (WEC) developed at Uppsala University is based on the concept of a heaving point absorber with a linear generator placed on the seafloor. The translator inside the generator oscillates in a linear fashion and is connected via a steel wire to a point absorbing buoy. The power production from this device is optimal when the translator's oscillations are centered with respect to the stator. However, due to the tides, the mean translator position may shift towards the upper or lower limits of the generator's stroke length, thereby affecting the power production. This effect will be severe if the WEC operates in an area characterized by a high tidal range. The translator may be stuck at the top or rest at the bottom of the generator for a considerable amount of time daily.

One of the solutions to this problem is to develop a compensator that is able to adjust the length of the connecting line. With an estimated weight of 10 tonnes of the connecting line and the translator, the use of a pocket wheel wound with steel chain was deemed suitable. Not being connected to an external power supply, the device needs a alternative local power supply to charge batteries that run the system. A hybrid system of solar photovoltaics (PV) and a small WEC was proposed to power the device and, based on the simulations for two different sea states, the hybrid system was found suitable for powering the device all year round. The experimental work carried out in the lab environment has shown that the compensator was able to lift the estimated load of the translator and to position the chain so that it follows the variations in the sea level from meteorological websites.

The second part of the thesis is a study on the wave energy potential in the Nordic synchronous grid. A model for the allocation of wave farms for four energy scenarios was developed, linearly weighted to the intensity of the wave energy flux. As an extension to this study, a net load variability study for a highly or a fully renewable Nordic power system was conducted. It involved four different intermittent renewable energy (IRE) sources: solar PV, wind, tidal power, and wave. The study shows that an optimal combination of IRE sources to replace fossil fuels and nuclear energy is possible from the perspective of net load variability.

Keywords: Wave energy, Tides, Wave Hub, Lysekil research site, Control system, Tidal compensator, Wave energy converter.

Mohd Nasir Ayob, Department of Engineering Sciences, Electricity, Box 534, Uppsala University, SE-75121 Uppsala, Sweden.

ISSN 1651-6214
ISBN 978-91-513-0627-8
urn:nbn:se:uu:diva-381169 (http://urn.kb.se/resolve?urn=urn:nbn:se:uu:diva-381169)

To my family

List of Papers

This thesis is based on the following papers, which are referred to in the text by their Roman numerals.

I Parwal, A., Remouit, F., Hong, Y., Francisco, F., Castel-lucci, V., Hai,L., Ulvgård, L., Li, W., Lejerskog, E., Bau-doin, A., **Ayob, M. N**., Chatzigiannakou, M., Haikonen, K., Ekström, R., Boström, C., Göteman, M., Waters, R., Svensson, O., Sundberg, J., Rahm, M., Strömstedt, E., Engström, J., Savin, A., and Leijon, M., "Wave Energy Research at Uppsala University and The Lysekil Research Site, Sweden: A Status Update", *Proceedings of the 11th European Wave and Tidal Energy Conference*, Nantes, France, 6-11 Sept., EWTEC 2015.

II **Ayob**, **M. N.,** Castellucci,,V., Terzi, M., and Waters R., "Tidal Effect Compensation System Design for High Range Sea Level Variations," *Proceedings of the 11th European Wave and Tidal Energy Conference,* Nantes, France, 6-11 Sept., EWTEC 2015.

III **Ayob**, **M. N.,** Castellucci, V., Göteman, M., Widén, J., Abrahamsson J., Engström, J., and Waters, R., "Small-Scale Renewable Energy Converters for Battery Charging," *Journal of Marine Science and Engineering*, vol. 6, no. 1, p. 26, Mar. 2018.

IV **Ayob**, **M. N.,** Castellucci, V., Abrahamsson, J., Svensson, O., and Waters, R., "Control Strategy for a Tidal Compensation System for Wave Energy Converter Device", *Proceedings of the International Offshore and Polar Engineering Conference*, Sapporo, Japan, 10-15 June, pp. 808–812. ISOPE 2018.

V **Ayob**, **M. N.,** Castellucci, V., Abrahamsson, J., and Waters, R., "A remotely controlled sea level compensation system for wave energy converters", Under revision for *MDPI Energies.*

VI **Ayob**, **M. N.,** Castellucci, V., and Waters, R., "Wave energy potential and 1–50 TWh scenarios for the Nordic synchronous grid," *Renewable Energy*, vol. 101, pp. 462–466, 2017.

VII Olauson, J., **Ayob**, **M. N.,** Bergkvist, M,. Carpman, N., Castellucci, V., Goude, A., Lingfors, D., Waters, R., and Widén, J., "Net load variability in Nordic countries with a highly or fully renewable power system," *Nature Energy*, vol. 1, no. November, p. 16175, Nov. 2016.

Reprints were made with permission from the respective publishers.

Contents

Abbreviations and Symbols

Abbreviation	Description
ECMWF	European Centre for Medium-Range Weather Forecasts
EMEC	European Marine Energy Centre
FEM	Finite element method
IRE	Intermittent renewable energy
OWC	Oscillating water column
PTO	Power take off
PV	Photovoltaic
RMSE	Root mean square error
ROV	Remotely operated vehicle
SMHI	Swedish Meteorological and Hydrological Institute
UU	Uppsala University
WEC	Wave energy converter

Symbol	Unit	Description
$\dot{E}_t$	W	Power from OWC
A_B	m^2	Cross-section of the buoy
A_a	m^2	Cross-section area of water piston
A_c	m^2	Cross-section area of tube
F_h	N	Hydrostatic force
F_e	N	Excitation force
F_{gen}	N	Generator damping force
F_{load}	N	Weight of the translator and buoy line
F_r	N	Radiation force
H_s	m	Significant wave height
R_a	Ohm	Coil resistance
T_e	s	Energy period
d_a	m	Water piston elevation
m_a	kg	Added mass
$\dot{z}$	m/s	Velocity of buoy
$\ddot{z}$	m/s^2	Acceleration of buoy

Symbol	Unit	Description
η_s		Efficiency of the compensator
ρ_{air}	kg/m^3	Air density
ω_a	rad/s	Motor speed
h	m	Water depth
A	m	Amplitude
I	A	Current
P	W/m	Power per meter wave crest
S	TWh	Energy
T	Nm	Torque
V	V	Voltage
g	m/s	Gravity acceleration
k	m^{-1}	Wave number
m	kg	Mass
p	W	Average power by PTO
t	s	Time
x	m	Position in space
z	m	Displacement of buoy
γ	Ns/m	Damping coefficient of the generator
η	m	Surface elevation
λ	m	Wave length
ρ	kg/m^3	Water density
σ		Standard deviation
ω	rad/s	Angular velocity

1. Introduction

In response to the oil crises in the 1970s, finding renewable energy resources to replace fossil fuels was a highly active field. However, after the oil price and economy stabilized, activities in this field waned until the 21st century, when the negative impact of finite-resource fossil fuels on the economy and the environment re-established the development and deployment of renewable energy. According to the *REN21-Renewables 2018-Global Status Report,* by the end of 2017 approximately 402 GW of solar PV and 539 GW of wind power were up and running and had seen an increase of 33% and 11%, respectively, compared to 2016 [1]. This expansion means that renewables now account for 70% of the net addition to the generation capacity of global power.

While wave energy technologies are generally still in the developmental and testing phases, and not comparable to wind and photovoltaic (PV) energy in terms of maturity and commercialization, the potential that ocean waves provide for generating electricity is undeniable. Consequently, there are now more and more efforts to push this technology forward. Several coastlines are licensed as development sites for offshore renewable energy. For example, the Lysekil research site located on the west coast of Sweden is a test site wave energy technologies, along with the Wave Hub and the European Marine Energy Centre (EMEC) in the UK.

As the technology for wave energy converters (WECs) matures, different concepts and techniques for improvements have been introduced. At Uppsala University (UU), the WEC concept is based on a heaving point absorber connected to a linear generator. Some of the studies that illustrate the improvements of this wave energy technology can be found in [2]–[6].

This thesis will present studies on improving WEC efficiency by compensating for the presence tides and their effect of decreasing energy absorption for certain wave energy converters. Although the wave energy concept of UU was considered in this thesis, the developed system is also applicable to other WEC technologies having a part fixed in position relatively to the seabed and a part that moves with the waves. The thesis will also involve a study on the wave energy potential in the Nordic synchronous grid and the possibility for achieving a power system that is highly or fully based on renewable resources from the perspective of net load variability.

1.1. Wave energy converter technology

There is a broad variety of wave energy technologies. Different methods have been used to categorize WECs. Based on their working principles, the technologies can be categorized as follows [7]:

1. Oscillating water columns (OWC)
   An OWC consists of a chamber with an opening to the sea. As the waves approach the device, the seawater is forced into the chamber and pressurizes the air inside the chamber. This air then escapes to the atmosphere through a turbine [8]. Conversely, when the water retreats, the air pressure in the chamber will go down and forces the air from the atmosphere into the chamber through the same air turbine. The turbine drives a generator for the production of electricity. An example of this device is the Wavegen Limpet, which is installed in Scotland and connected to the national grid.

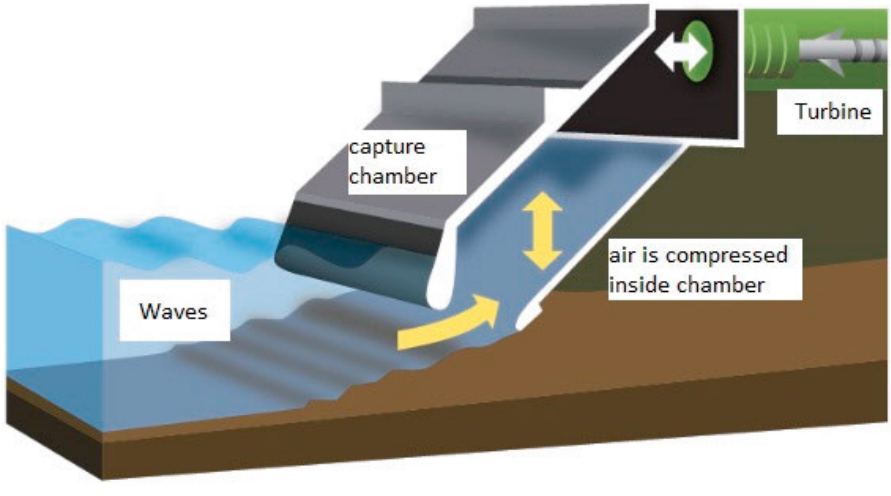

Figure 1.1. The Wavegen Limpet OWC device. Figure adapted from [9].

2. Oscillating bodies
   As the name suggests, the WEC consists of oscillating bodies that move relative to eachother. They are usually installed offshore where the waves are more energetic. The technology can be further classified into several subcategories, including single-body heaving buoys, two-body heaving systems, fully submerged heaving systems, pitching devices, bottom-hinged systems, and many-body systems [7]. The wave energy devices developed at UU are categorized as single-body heaving buoys.

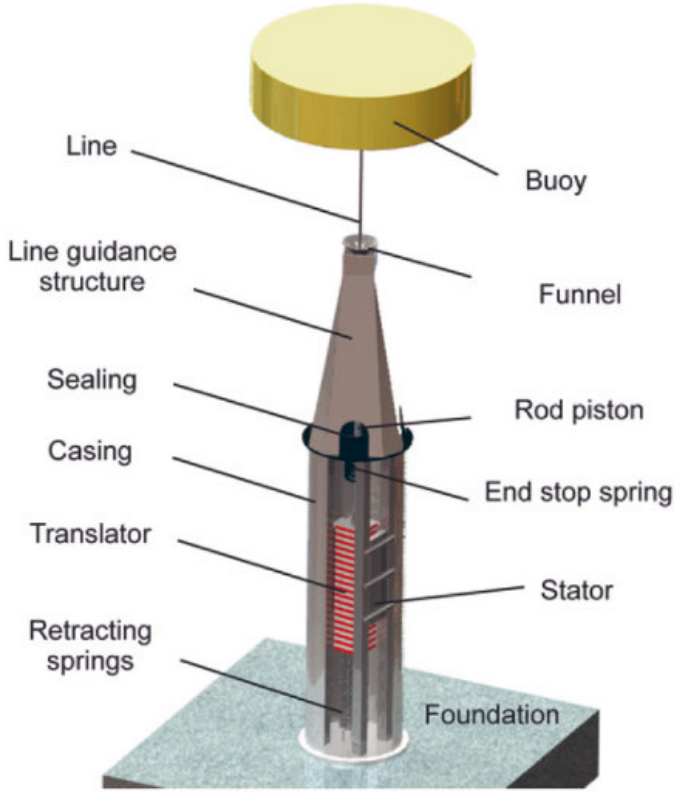

Figure 1.2. The Uppsala University WEC. Figure by courtesy of Magnus Rahm [10].

3. Overtopping device
   An overtopping device is a partially submerged WEC, forcing the waves together and up a ramp into a reservoir with a water level that is higher than the surrounding ocean. The kinetic energy from the waves are thus converted into potential energy. The water from the reservoir returns to the sea through a turbine driving a generator for electricity production. An example of this device is the Wave Dragon, which was developed in Denmark [11]

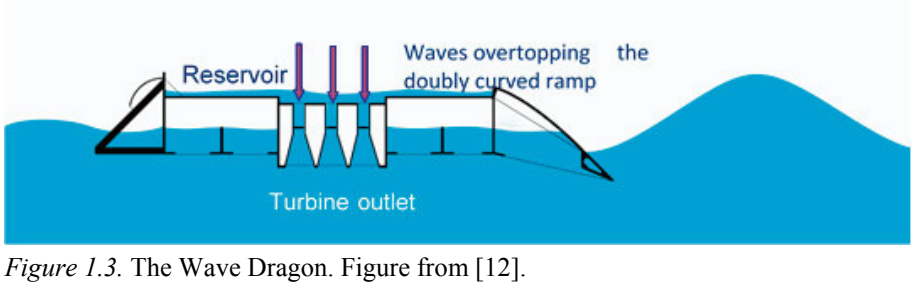

Figure 1.3. The Wave Dragon. Figure from [12].

1.2. The Lysekil project

The Lysekil wave energy research site is located on the Swedish west coast, about 100 km north of Gothenburg. Since 2002, the wave energy research group at Uppsala University (UU) has developed technology to convert ocean wave energy into electrical energy. The first full-scale deployment was in 2006. The wave climate at the site has been studied by Waters et al. [13], who concluded that the mean energy flux is approximately between 2.8 kW/m and 5.2 kW/m at different locations on the Swedish west coast.

The wave energy research at UU covers a wide range of topics as illustrated by Paper I:

1. Wave energy generator and buoy
   The first offshore generator, known as L1, was installed in 2006 [14]. The generators following the L1 focused on improvements on rated power, survivability, cost and making the designs suitable for series production. The latest generator was the L12 model with 3 phases and 8 sides and a weight of around 9800 kg.

2. Marine substation
   The marine substation is installed on the seabed and is connected to the WECs with underwater connectors. The AC level from the WECs is converted to DC at the marine substation. The DC is then inverted back to AC and transmitted 3 km to shore by a subsea power cable to a measuring station on a nearby island.

3. Measuring station
   The measuring station is equipped with a resonance circuit and a DC chopper for active control of the DC voltage. The resonance circuit serves to control the damping of the generator, thus optimizing the power production. The measuring station is also facilitated with a transformer 1/11 kV and necessary protection for grid connection.

4. Auxiliary system
   The control system, measurement system, and communication system are also equally important research topics at UU research group. For some aspects of the control strategy and the communication system, the reader is referred to previous studies [15]–[18].

5. Remotely operated vehicle (ROV)
   The deployment of large arrays of WECs and other underwater facilities calls for an appropriate method for handling safety issues and to reduce operational cost. For this reason ROV have been studied, especially with regards to the underwater cable connections [19], [20].

6. Wave power farms
   The study of large WECs arrays and wave farms is also an important part of the wave energy research at UU. Different control strategies and park configurations have been tested to analyze the interaction between the buoys and the power production from wave parks [21]–[23].

7. Environmental studies
   The deployment and operation of a wave energy farm will impact the surrounding environment. In order to assess the sustainability of the technology developed, studies on the impact of the technology on marine mammals and fish behavior are of high importance. Hence, it is also one of the main focus research areas at UU [24][25].

8. Grid connection
   An automatic grid connection control system is studied to connect and disconnect wave farms. Ref. [22] describes the control procedures at the substation stage, involving damping control and protection of the WECs, power quality control, fault handling, and grid synchronization.

9. Tidal compensator
   A tidal compensator system is an approach to minimizing the adverse effects of mean sea level changes, mainly due to tides. The first tidal compensator developed at UU, dimensioned for the Swedish west coast and able to compensate up to 1 meter, was tested near the shore of Lysekil in 2014 [26]. This thesis will focus on the next-generation tidal compensator dimensioned for a tidal range of up to 8 meters (Papers II, III, IV and V).

1.3. Aims of the thesis

This thesis presents the development of a sea level compensator that can be used to keep the generator of WECs in optimal working conditions in regions with tides. A prototype of the device was constructed and laboratory experiments were performed to analyze the control, communication, and power consumption of the device. The wave and tidal conditions at Wave Hub have been studied as a reference case for the development of the self-powered tidal compensator.

This thesis also presents an analysis of the wave energy potential in the Nordic countries for a number of different scenarios. Furthermore, the potential for a highly or fully renewable power system in the Nordic countries, through different mixes of IREs, is also presented. The simulations and data

analyses were carried out using MATLAB, and the data on wave characteristics for a period of 10 years (2005-2014) were obtained from the European Centre for Medium-Range Weather Forecasts (ECMWF) [27].

2. Theory

2.1. Tides

This chapter will briefly discuss the definition of tides and how different types of tides arise. Tides are the result of the gravitational forces by the moon and the sun on the sea combined with the earth's rotation generating a centrifugal force. The point on the earth closest to the moon experiences a greater gravitational pull compared to the opposite side on the earth. The orbit of the moon around the earth is elliptical, which results in variation in the tide-producing force [28]. When the moon is closest to the earth it is called perigee, and when the moon is furthest away from the earth it is called apogee.

For a simple explanation, the following figure will consider the case where the inclination of the sun and the moon are both zero. The highest tide is called spring tide, Fig. 2.1 (top), and it appears when the sun and moon are aligned with the earth. Fig. 2.1 (bottom) shows the opposite situation where the forces from the sun and moon are most separated. This happens when the sun and the moon act at a right angle which means that the solar and lunar tides are out of phase. This phenomenon is called the neap tide.

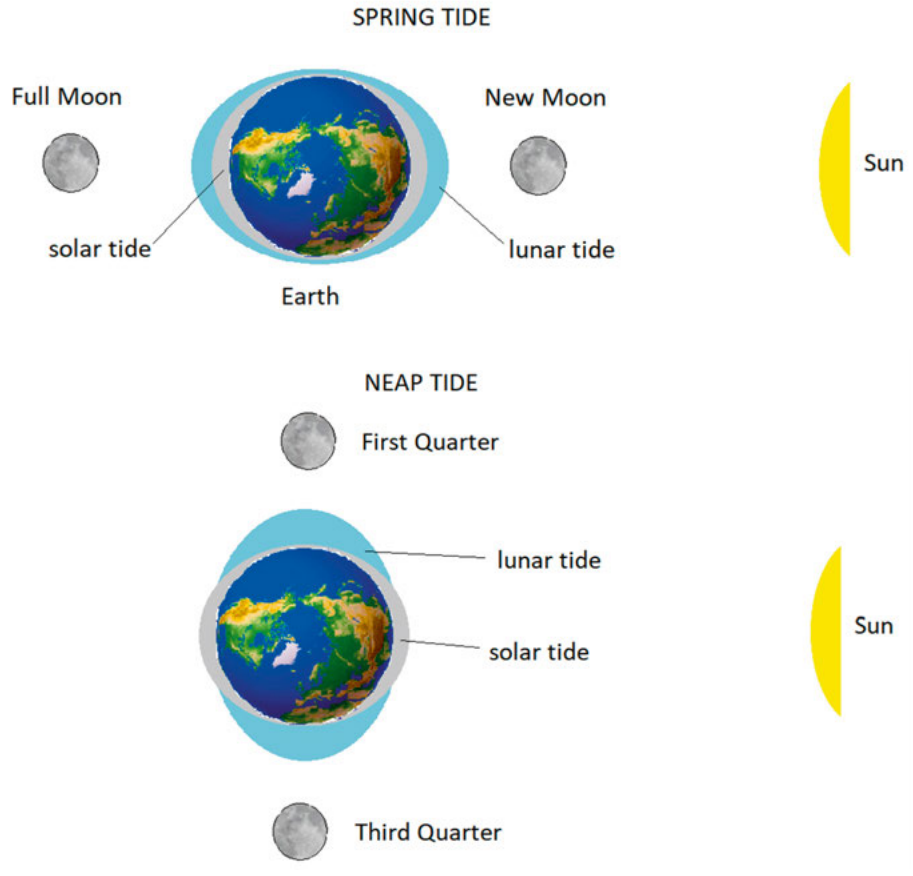

Figure 2.1. Illustration of the formation of tides with four different positions of the moon. The inclination of the sun and the moon relative to the earth are assumed zero.

The moon revolves around the earth once every 27.3 days, in the same direction as the earth rotates on its axis. As the earth completes its rotation in 24 hours, the period of the earth's rotation with respect to the moon is 24 hours and 50 minutes, also known as a lunar day. In theory, except at the highest latitude, the earth will rotate through two tidal bulges and experience two equally high and two equally low tides per lunar day. The rise and fall of the sea level on earth are however strongly influenced by the topography and the distribution of the continents - therefore, different regions of the world will experience different tidal cycles [29]. In general, these cycles can be described as semi-diurnal, diurnal, and mixed tidal cycles. A semi-diurnal cycle consists of two high and two low tides during the lunar day. The tidal period is 12 hours and 25 minutes (from high tide to the next high tide). A diurnal tide consists of only one high and one low tide each day. The tidal period is 24 hours and 50 minutes. Mixed tides can have two high tides and two low tides

with different sizes each lunar day. The illustration of these phenomena is given in Fig. 2.2.

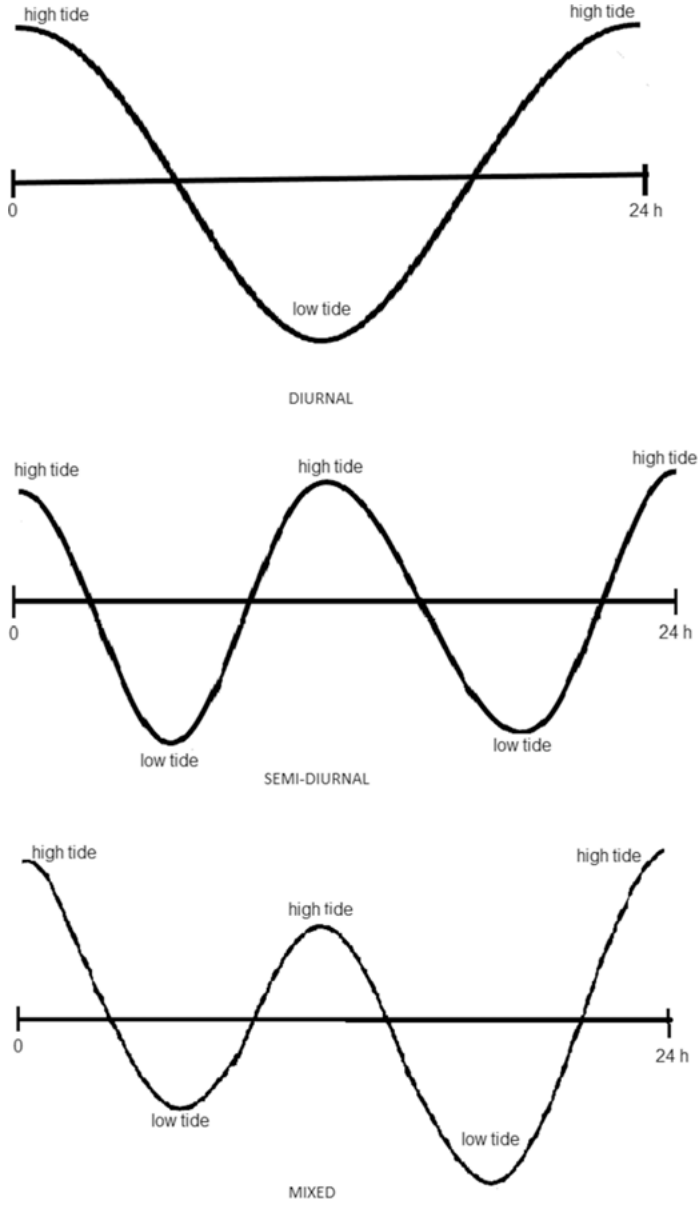

Figure 2.2. Types of astronomical tides. A diurnal tide is characterized by one high and one low tide. A semi-diurnal tide is characterized by two high and two low tides. A mixed tide may consist of a combination of two different high and two different low tides.

2.2. Waves

Water waves can be categorized into three types: wind and swell waves, wind surges, and sea waves of seismic origin (tsunamis) [30]. The most common waves in the ocean are wind and swell waves. When the wind blows across the surface of the ocean, energy is transferred to the water creating surface currents and waves. After the wind ceases to blow, created wind waves will continue to propagate and are called swell waves. In other words, swell waves consist of wind-generated waves that are not affected by the local wind at that time. In general, the waves used by WECs to harness energy are wind and swell waves [31].

2.2.1. Regular and irregular waves

For a parallel plane wave, the surface elevation can be described in the time domain as

$$\eta(x,t) = A\cos(kx - \omega t + \theta), \tag{2.1}$$

where A is the amplitude, x is the position in space in the direction of the wave propagation, t is time, ω is the angular frequency, θ is the phase, and $k = \frac{2\pi}{\lambda}$ is the wave number with λ being the wavelength.

In the dispersion relation, the angular frequency and the wave number are related as

$$\omega^2 = gk\tanh(kh), \tag{2.2}$$

where g is the gravity acceleration and h is the water depth.

Fig. 2.3 illustrates a regular wave consisting of a single-frequency sinusoidally shaped wave. In reality, however, the waves are irregular and can be represented as a linear superposition of sinusoidal waves of different amplitudes, frequencies, and phases.

In wave energy, the preferred representative wave height is the so-called significant wave height denoted as H_s, which is the average height of the one third-highest waves during a studied time frame, or as four times the square root of the area under the wave spectrum curve, $H_{m0} = 4\sqrt{m_0}$. The wave energy period, T_e, is the ratio of the first negative moment of the spectrum to the zeroth moment of the spectrum:

$$T_e = \frac{m_{-1}}{m_0}. \tag{2.3}$$

For a valid deep water approximation [32], the available power per meter wave crest can be represented as

$$P = \frac{\rho g^2}{64\pi} H_s^2 T_e, \tag{2.4}$$

where ρ is the density of sea water.

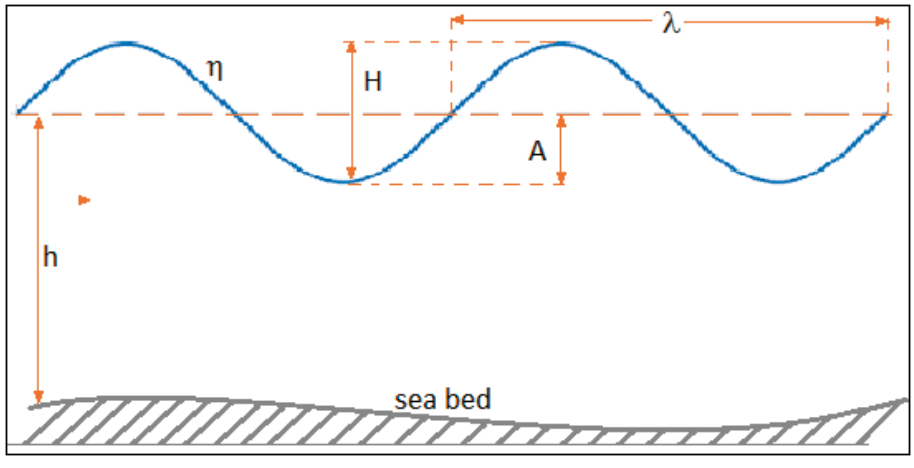

Figure 2.3. A regular wave with a depth h, where H is the wave height, A is the amplitude, and λ is the wavelength.

2.2.2. Wave energy extraction

"In order for an oscillating system to be a good wave absorber, it should be a good wave generator" [33].

Floating point-absorbing WEC

A heaving point absorber connected via a steel wire to a linear generator (see Fig. 1.2) can be modeled as a two-body system in the time domain [34]. For further simplification, the buoy and the translator can be assumed to be rigid (the case of a small WEC is described in Paper III). A simplified model of a linear generator connected to a partially submerged buoy moving in heave can be represented as

$$m\ddot{z} = F_e + F_r + F_h + F_{gen}, \tag{2.5}$$

where m and z are the total mass of the moving parts and the buoy elevation, respectively; F_e, F_h, and F_r are the excitation, the hydrostatic, and the radiation force, respectively, acting on the floating buoy; and F_{gen} is the damping force from the generator. The hydrodynamic force is computed based on the linear potential flow theory [35]. The excitation force is

$$F_e(t) = f_e(t) * h(t), \tag{2.6}$$

where $f_e(t)$ is the impulse function of the buoy. The radiation force, F_r, is then defined as the convolution product between the radiation impedance [4] and the vertical velocity, $\dot{z}$. F_h is the buoyancy stiffness and is proportional to $z(t)$, while F_{gen} is the generator force with the damping coefficient γ

$$F_{gen} = -\gamma \dot{z}(t). \tag{2.7}$$

In the frequency domain, the relation between the wave amplitude , $\hat{h}$, with the buoy elevation, $\hat{z}$, can be represented as

$$\hat{H}(\omega) = \frac{\hat{f}_e}{-\omega^2(m + m_a) + i\omega(\gamma + R) + \rho g A_B}, \tag{2.8}$$

where $\hat{f}_e$ and R are the hydrodynamic parameters of the buoy, m_a is the added mass, and A_B is the cross-section of the buoy. The elevation of the buoy, z is the result of the convolution of the transfer function H with the wave amplitude h. In the time domain, $z(t)$ is equal to

$$z(t) = H(t) * h(t). \tag{2.9}$$

The average wave power extractable by the power take off (PTO) is given in Eq. 2.10. In the time interval [0,t],

$$p(t) = \frac{1}{t}\int_0^t \gamma \dot{z}^2 \, dt\,. \tag{2.10}$$

Oscillating water column (OWC) WEC

With regards to the many different wave energy concepts briefly discussed in the previous section, OWC WECs can be considered as one of the simplest. OWC WECs are also considered to be the first wave energy devices that were successfully deployed into the sea [36]. The first OWC was developed by Yoshio Masuda, who created a navigation buoy powered by wave energy. In general, the OWCs can be further classified into two different types: offshore OWCs and onshore OWCs. The Wavegen Limpet illustrated in section 1 is an onshore device. The offshore OWCs are usually depicted as floating on the sea surface and moored to the seabed. Fig. 2.4 illustrates the main parts of a floating OWC.

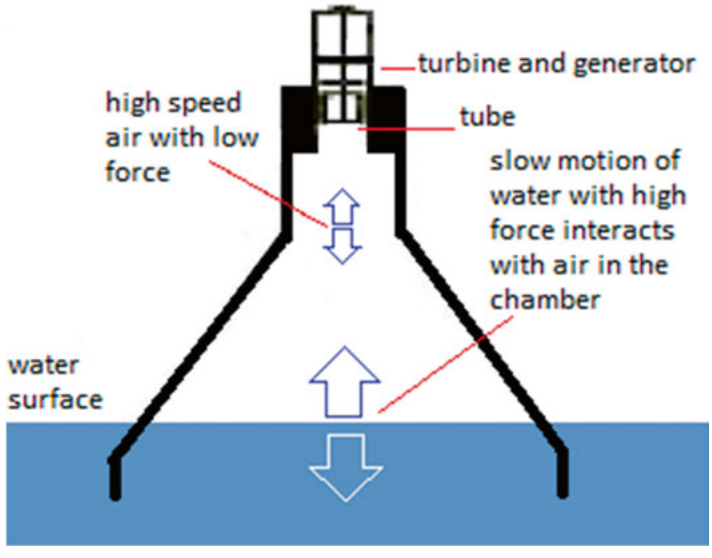

Figure 2.4. An illustration of a floating OWC WEC.

The theoretical approach to the OWC in Paper III is simplified in order to calculate a first order approximation of the electrical energy that can be converted for the studied application. The following simplifications have been used: (1) The volume of the chamber is considered to be cylindrical and (2) the presence of the turbine and the generator and their respective efficiencies were not considered. For a cylindrical OWC, the water column moves up and down in the chamber following the waves. The water in the chamber acts as a piston compressing and expanding the air inside the chamber and forcing the air through the tube and turbine.

The maximum power absorption from an OWC can be estimated from the concept of a control volume [37]. The air velocity passing the tube is obtained from a mass balance equation. Based on the shape of a cylindrical chamber, the volume of air is given at time t as

$$V_a(t) = Vc - Ad(t), \tag{2.11}$$

where V_a, Vc, A, and d are the control volume, the chamber volume, the cross-section of the chamber and the water piston elevation inside the chamber. By assuming that the fluid (air in this case) is incompressible, the rate of air volume passing the tube can be presented as

$$\dot{V}_a(t) = \frac{-\mathrm{A}\mathrm{d}d(t)}{\mathrm{d}t}. \tag{2.12}$$

By considering the Betz limit [38] of $16/27$ as the maximum extraction of kinetic energy from moving air, the power production, $\dot{E}_t$ from a simplified model of an OWC can be presented as

$$\dot{E}_t = \frac{1}{2}\frac{16}{27}\dot{m}_a v^2 = \frac{-8\rho_{air}\dot{d}_a(t)^3 A_a^3}{27A_c^2}, \tag{2.13}$$

Where $\dot{m}_a$, v, ρ_{air}, d_a, A_a, and A_c are the mass flow rate, the air speed at the tube, the air density, the water piston's vertical position, the piston's area, and the tube's cross-section, respectively.

3. Method

3.1. Experimental work in Lysekil

The wave energy research group at UU runs an advanced wave power testbed 2 km offshore near the town. Lysekil on the Swedish west coast. Since 2005 a large number experiments have been conducted at the site on an extensive amount of large scale prototypes - e.g. a total of 12 ten meter high and 50 tonnes prototype wave power plants, 2 marine sub-stations, numerous cables for power, measurements and control, an ob-servation tower, buoys for environmental impact studies, force and wave climate studies. This is the research group's lab, and it is run by PhD-students and senior researchers. The research site and the experi-ments are a foundation for the research group's studies, but maintaining and expanding it, and performing experiments is both expensive, time consuming and risky. The only way to maintain the research site is if all researchers and PhD students help out. The author has spent count-less days working at the research site and has thus contributed to the overall research of the UU wave energy research group. The overall work of the research group can be hinted in Paper 1 but is otherwise not seen in this thesis due to the focused nature of the author's research.

A majority of the design and development work takes place at UU's facilities in Uppsala. However, the later stages of the deployment and experimental work takes place in Lysekil on the Swedish west coast. Fig. 3.1 shows some of the experimental work on the West coast that the author has been responsible for. The experiments took place 2 km offshore at the Lysekil research site; on the island Härmanö, where the measurement cabin and the grid connection point are; at the Lysekil Harbor; and at the Seabased AB production plant.

Figure 3.1. (a) Deployment of 3 km power cables from the Lysekil research site to the measurement cabin on Härmanö Island. A boat with a small crane facilitated the deployment. (b) Cable splicing and cable connection sealed with water-tight compounds. (c) The linear generator L10 and the marine substation ready to be transported to the deployment site. (d, e) Work on the marine substation: (d) view from inside the substation, (e) outside the substation: mounting of cables and leakage inspection with the base submerged in a water basin. (f, g) Deployment of power and signal cables 300 m from the observation tower (f) to the deployment site of the WECs, with (g) cable reels mounted on a small barge, towed by a boat.

3.2. High-range tidal compensator

From the knowledge and lessons gained from simulations, the laboratory experiments and the sea tests of the UU's WECs on the Swedish west coast [16], [39]–[44], the research focus was broadened to include the study of the adaptability of the UU's WECs to different sea climates. Among others, the adaptation of the technology to higher mean sea level changes was investigated. As briefly described in Section 2.1, tidal variations can be experienced in most parts of the oceans on the planet. Different locations and continents will experience different tidal levels. As the tidal variation at the Lysekil research site is usually no larger than 0.2 meters and only rarely up to 0.8 meters, the tidal variations at Lysekil have been shown to not have a significant negative impact on the power production of the WEC. However, this will not be the case if the tidal range is higher as, for example, at the Wave Hub - one of the exciting testbeds WECs due to its comprehensive support for offshore renewable energy technology. The Wave Hub is located off the west coast of Cornwall, with a tidal variation registered at the Newlyn Tidal observatory, 22 km to the south, of 6.6 meters [45]. The first compensator system from Uppsala, for tides of approximately 1-2 meters, was developed and tested in Lysekil in 2015 [26]. The next section will describe the development and testing of a high-range sea level compensator (Papers II, III, IV, and V).

3.2.1. Hybrid renewable energy system for battery charging

As the system is designed to be a self-powered device, a reliable battery charging system is a necessity. A small-scale renewable energy converter was selected to power the device and to charge the batteries [46] (Paper III). The power produced by a hybrid system consisting of a small WEC with solar PV was studied. Since the system would be mounted on the main buoy, the size of the small WEC was set to 35 cm in diameter as to not limit the operation of the WEC's 5 m diameter point absorbing buoy. Fig. 3.2 illustrates how the small WEC can be installed on the main WEC.

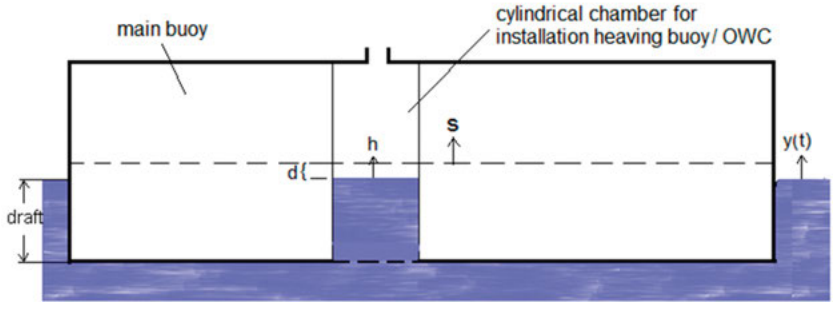

Figure 3.2. An illustration of the cross-sectional view of a cylindrical buoy. The small cylindrically shaped tube close to the center of the buoy is a possible installation slot for a small WEC (OWC or small point absorber) that can power the sea level compensator.

The analysis of the energy potential for the output from the small WEC was performed based on two different sea states at the Wave Hub, whereas the analysis of the solar PV energy produced was based on the data obtained from PVGIS [47]. The monthly solar irradiation at the Wave Hub is shown in Fig. 3.3.

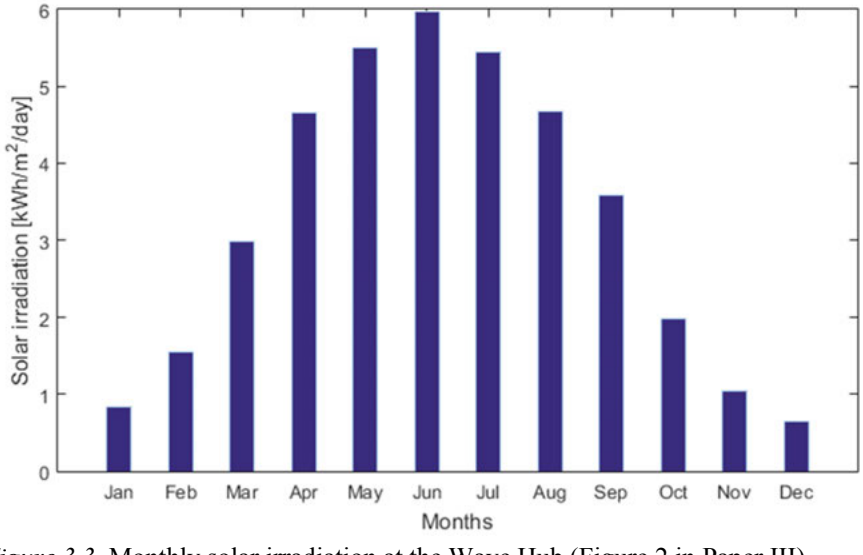

Figure 3.3. Monthly solar irradiation at the Wave Hub (Figure 2 in Paper III).

The power production was calculated based on two different WEC types, an OWC and a heaving point absorber (referred to as SB in Paper III). Both the OWC and the SB were simulated with dimensions suitable for installation in the cylindrical chamber on the main buoy.

3.2.2. Mechanical design

The mechanical design of the compensator is shown in Figure 3.4. It was dimensioned based on results obtained from simulations using SolidWorks. The simulations include displacement, strain, and stress tested with internal and external loads. The von Mises yield criterion was used as the analysis criteria. Table 3.1 shows some properties of the material selected for the support structure.

Table 3.1. Properties of the support plate.

Properties	**Unit**	**S355**	**EN1.4404**
Elastic modulus	MPa	210000	200000
Mass density	kg/m^3	7800	8000
Tensile strength	MPa	450	600
Yield strength	MPa	275	400

The pitch diameter of the wheel shown in the figure is 32 cm, and the axis diameter is 16 cm. Fig. 3.5 shows the completed assembly of the main parts of the compensator for the experiments in the lab.

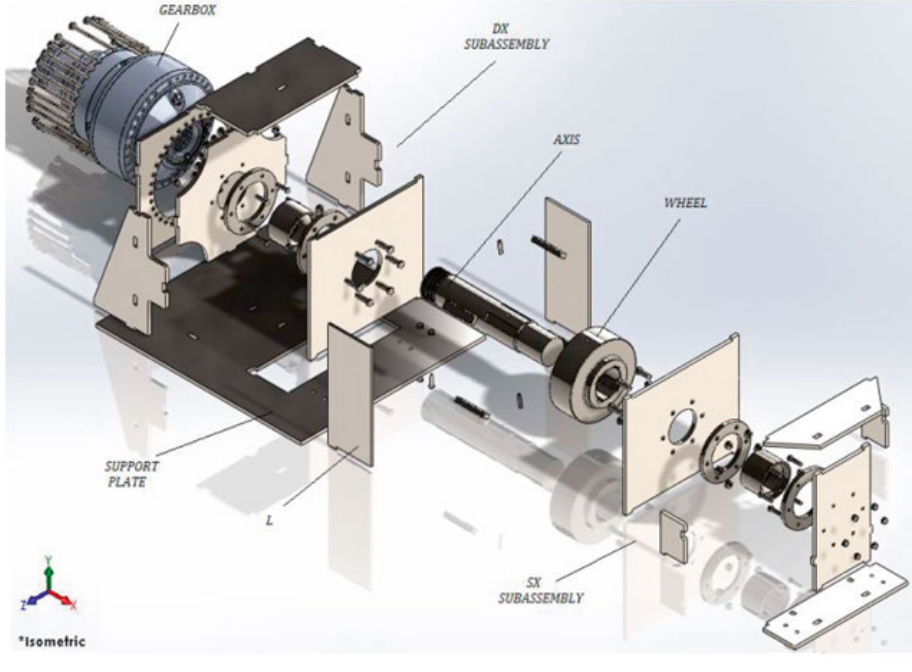

Figure 3.4. An enlarged view of the mechanical parts of the tidal compensator.

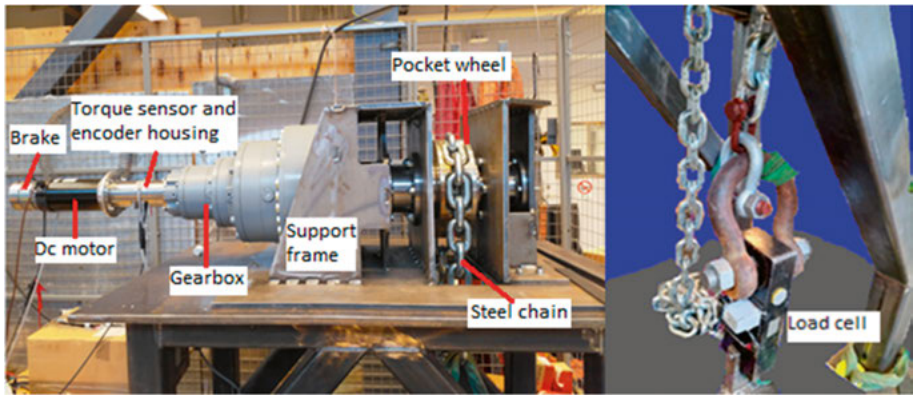

Figure 3.5. (left) The compensator setup on a steel table. (right) The steel chain pulls a load cell welded to the floor (Figure 7 in Paper V).

3.2.3. Communication and control

In Fig. 3.6, the communication and control flow is shown with a simplified block diagram. The input parameter of the system is the sea level collected online from the website of the Swedish Meteorological and Hydrological Institute (SMHI) [48]. The primary server is placed on land at UU. The server acts as the main component of the communication and control system. The server obtains sea level information from the SMHI and makes a prediction of the present sea level (see Paper V) which is necessary because the observational data obtained from the SMHI has a lag of 1 to 2 hours. The server and the compensator exchange command and log data via the cloud service cloudAMQP [49] based on RabbitMQ. The advantage of using this cloud service lies in its simplicity. The communication between the server and the compensator is asynchronous, thus avoiding the polling for data availability.

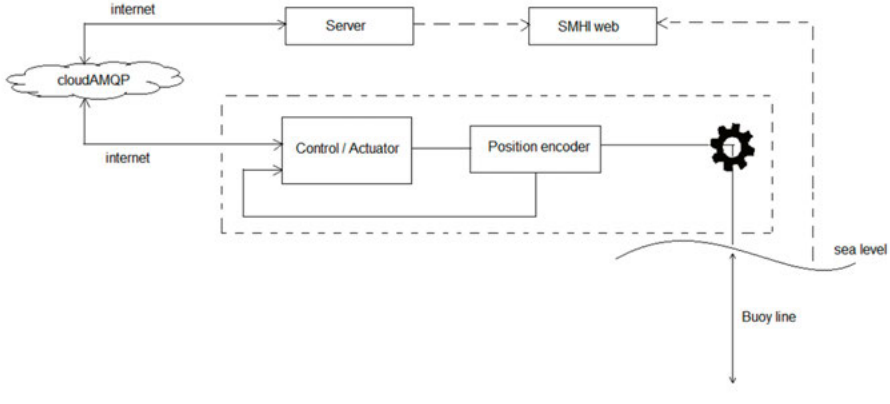

Figure 3.6. The control flow of the sea level compensation system (Figure 1 in Paper V).

3.2.4. Equipment

Fig. 3.7 shows an overview of the compensator's main components. The main parts include the power supply, the communication system, the sensors, the controller, and the mechanical system. The main controller of the system is an Arduino Mega 2560 [50]. The input to the Arduino is coming from the sensors, and the output from the Arduino is the control signal for the DC motor (speed and directional control) and brake. The Raspberry Pi (RPi) is used primarily for 3G/4G communication between the server and the compensator. Acting as a small computer, the RPi is a convenient method for multitasking applications involved in communication, data logging, and monitoring. More details about the components are shown in Fig. 3.7 and have been discussed in Paper IV. The compensator system was designed to operate as a self-powered device. A hybrid RE system is necessary to charge the battery, as mentioned in Section 3.2.1 and further discussed in Paper III.

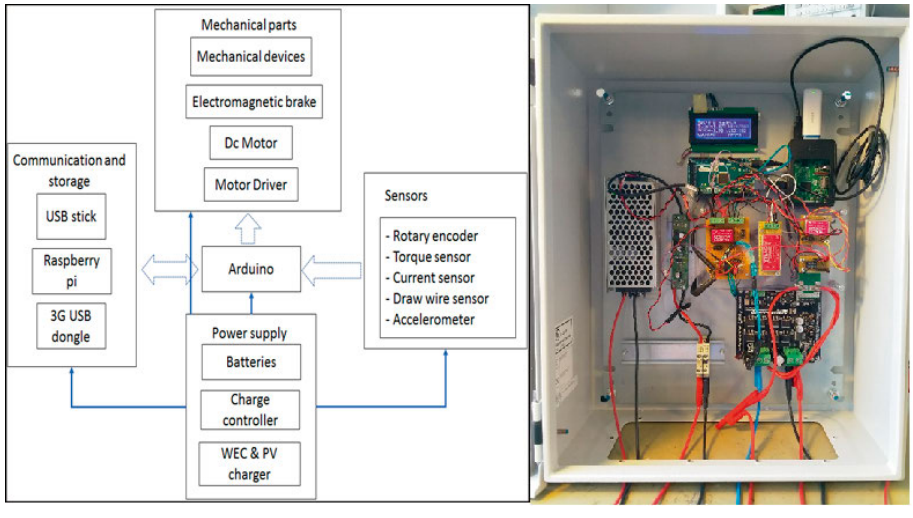

Figure 3.7. Left: An overview of the compensator's main components [51]. Right: The electronic components installed in a metal cabinet.

3.2.5. Experimental test

A static- and a dynamic-load test was performed in the lab environment to (i) evaluate the power consumption and the positioning of the compensator when lifting different loads and (ii) to characterize the motor e.g. with regards to its efficiency. In the dynamic test (see Paper IV), two pairs of spring stacks were compressed, and the amount of force exerted (lifting force of the compensator) and the vertical position of the chain were measured. One of the springs is rated for compression up to 10 kN and different stack arrangements will change the total spring's constant. For this experiment we have arranged the

springs so that it would be possible to measure up to 40 kN if the springs are fully compressed. In the experiments, a steel bar attached to the compensator chain was used to compress the spring stack up to a maximum of 35 kN. The springs were not fully compressed for safety reasons. Several measurements were made with the same setup in order to achieve good accuracy of the measurements. The details of this setup is available in Paper IV. The power consumption and the estimated control parameters obtained from this dynamic-load test gave information on how to design the control system for the compensator. In the steady state, turning the motor at a constant speed, ω_a, with the voltage, V, and the corresponding current, I, can be represented as

$$(VI - I^2 R_a)\eta_s = T\omega_a|_{T\ at\ \omega_a} + F_{load} v|_{v\ at\ \omega_a}, \tag{3.1}$$

where η_s, F_{load}, T, v, and R_a are the efficiency of the system, the estimated load of the translator and the buoy line (100 kN), the torque, the linear speed of the chain at ω_a, and the coil resistance, respectively.

Furthermore, the static test was used to calibrate the system and test the capacity of the compensator to lift 100 kN, the estimated weight of a real full scale translator. The setup is shown in Fig. 3.5.

The real-time chain positioning and communication control system was evaluated by performing a dynamic test without the load. The positioning of the compensator was set according to the sea level at Brofjorden, an observation station located on the west coast of Sweden. The information was accessed online from the SMHI. Fig. 3.6 shows the simplified block diagram of the communication and control flows.

3.3. Energy potential in the Nordic countries

The study in Paper VI estimates the wave energy potential along the coast of the Nordic countries. A model for the allocation of wave farms was developed where the probability of a site being chosen is linearly weighted to the intensity of the wave energy flux at the site. The model was used to generate four targeted energy scenarios of 1 TWh, 3 TWh, 10 TWh, and 50 TWh yearly with the purpose of supplying wave energy to the Nordic synchronous grid.

The wave farm allocation model adds one wave park at a time until the targeted energy scenario is reached. From the energy flux calculated, it was assumed that 25% of the available energy during the 90% least energetic sea states is convertible into electrical energy – i.e. a cap was placed on the energy absorption. The model for the energy scenario can be represented as

$$S = \sum_{R}^{n} \hat{P} \times 4.38 \times 10^6 \tag{3.2}$$

where S is the target energy for a year in TWh, $\hat{P}$ is the harnessed mean energy flux at coordinate R, and n is the total number of points for generating the scenario. Fig. 3.8 shows an example of the cap set to the energy flux for a location at lat. 58.35° and long. 11.37°.

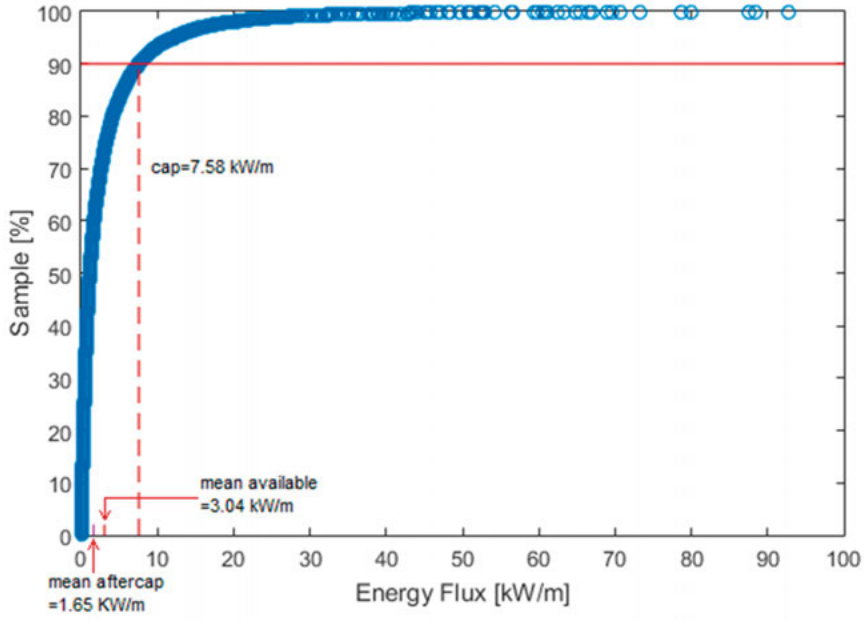

Figure 3.8. The cumulative appearance of the energy flux for ten years (lat. 58.35° and lon. 11.37°) (Figure 1 in Paper VI).

3.4. Renewable energy variability

Electrical power systems can, in general, be divided into 3 parts: (1) the generators that supply the power, e.g. hydro-, wind-, solar-, wave-, nuclear-, and thermal generators (2) the transmission system that delivers the power from the generators to load centers, and (3) the distribution system that transmits power from load centers to the consumers such as households, electrical transportation systems, and industries. The total electric power consumption is called load and it varies on different time scales – from hours to seasons. Paper VII is a study of *net load* variability in the complete Nordic synchronous power system. The net load variability is defined as the total load minus the intermittent renewable energy sources (IRE), nuclear and thermal energy. As an extension of the study carried out in Paper VI, it involved four different intermittent renewable energy (IRE) sources, which are solar PV, wind, tidal power, and wave.

The study aimed at producing an optimal combination of IRE by separating the variability into different frequency bands. The four IREs studied were

modeled in terms of hourly values of generated power (TWh/h). As described in detail in Paper VII, the raw load and IRE signals were separated into four frequency components: long-term (LT, > 4 months), mid-term (MT, 2 weeks to 4 month), mid/short-term (MST, 2 days to 2 weeks), and short-term (ST, < 2 days) components. The study on different timescales is important because it relates to the challenges of a power system - such as the ramping capability of the power system on hourly or subhourly timescales, hydropower planning on intermediate timescales, and seasonal energy storage planning.

The focus of the study was on the variability on the different timescales with various mixes of IREs for projecting different energy scenarios from a highly renewable to a fully renewable energy system. In the highly renewable scenario, new renewables replaced old IREs, fossil energy sources, and 30% of the nuclear production - accounting for 20% of the load. In the fully renewable scenario, a complete replacement of nuclear, fossil, and old IRE resources was assumed – resulting in IREs accounting for 36% of the load. For each scenario, predefined mixes (Mix 1 and Mix 2) and an optimized mix of IREs were considered. Mix 1 is comparable to the mix used today, while Mix 2 is more futuristic with a maximum tidal production of 3 TWh/year and the remaining made up of 40% PV, 40% wind, and 20% wave. The optimization was done to reduce the standard deviations of the net load for each frequency component as well as the total standard deviation – i.e. to find optimal mixes of IREs. The following equation defines the total standard deviation:

$$\sigma_{raw} = \sqrt{\sigma_{LT}^2 + \sigma_{MT}^2 + \sigma_{MST}^2 + \sigma_{ST}^2}, \tag{3.3}$$

where σ is the standard deviation.

4. Results and Discussion

4.1. High-range tidal compensator

4.1.1. Power from OWC

The vertical motion of the water piston, d, inside the chamber (see Fig. 3.2) is the result of the interaction between the ocean wave and the main buoy. The water piston acts as the driving force for the OWC. The power production from the OWC was calculated by Eq. 2.13. The power output from an OWC is significantly influenced by the chamber diameter and the outlet diameter. In order to simplify the calculation, the following ideal behaviors of the system were assumed in the simulation:

- Incompressible fluid
- Maximum kinetic energy conversion based on the Betz limit
- The absence of the turbine in the outlet

In reality, the vertical elevation would be smaller because of the reaction force of the chamber acting in the opposite direction to the water piston when energy is extracted by the turbine. However, even with the ideal case assumptions, the OWC produces an average power of maximum 5.3 W which is too little to power the device. The average power needed to charge the batteries is approximately 37.7 W.

4.1.2. Power from the heaving point absorber

The power extracted by the PTO depends on the damping coefficient, γ, and the SB's vertical velocity, $\dot{z}$. From the simulations of the small WEC for two difference sea states, it was decided to set $\gamma = 600\ Ns/m$ in order to prioritize the energy absorption for the most common sea states at the Wave Hub. The resulting average power generation is 32.4 W.

4.1.3. Simulation and experimental results

The main part of the tidal compensator was designed and installed on a steel structure for testing. Several tests were performed to evaluate the compensator in terms of control and communication and the capability of lifting the esti-

mated load of the translator. The strength of the support structure for the compensator was evaluated with a finite element method (FEM) using SolidWorks. Table 4.1 shows the result of the von Mises criteria and the yield strength of the material. The results were based on the test load of 500 kN.

Table 4.1. Von Mises test on the support structure

Support structure part	Material type	Material's yield strength (MPa)	Force/Torque applied	Max. von Mises stress (Mpa)
Gearbox's support	S355	275	3 kN 80 kNm	3 75
Bearing's support (load support)	EN1.4404	400	250 kN	252

The result of the von Mises criterion test shows that the maximum stress on the support structures is well below the material's yield strength. In the case of commercial applications, one should consider strengthening the bearing support in order to protect the structure against fatigue damage.

The energy provided from the small WEC to the system, as discussed in Paper III, is around 900 Wh per day. When dimensioning the small WEC, this number was considered the minimum needed to run the system and to charge the batteries. The control strategy is designed to account for this energy con-straint - compromising between the desire for small errors when positioning the compensator and energy use since higher accuracy of the positioning means more adjusting time of the compensator and a higher consumption of energy.

Fig. 4.1 shows the result of the compensator positioning for a duration of 2 days. The operation was performed without the load (translator) attached to the chain to evaluate the control and communication. The result shows that the compensator position (red color) fits reasonably well to the online obser-vation data (orange color). The position of the compensator was the result of a continuous 2-hour extrapolation of the observational data at Brofjorden.

While the experimental test on the compensator was conducted to follow the tidal data at Brofjorden online, the simulation test to evaluate the adaptation of the system at Wave Hub was done offline (one-year data). The evaluation of the proposed system's performance was based on the positioning error and the power consumption of the compensator (Fig. 4.2). As for the control strategies, the performance of the device was simulated with four different adjustment time intervals: 15, 30, 60 and 120 minutes. This time interval is the period between each adjustment of the compensator.

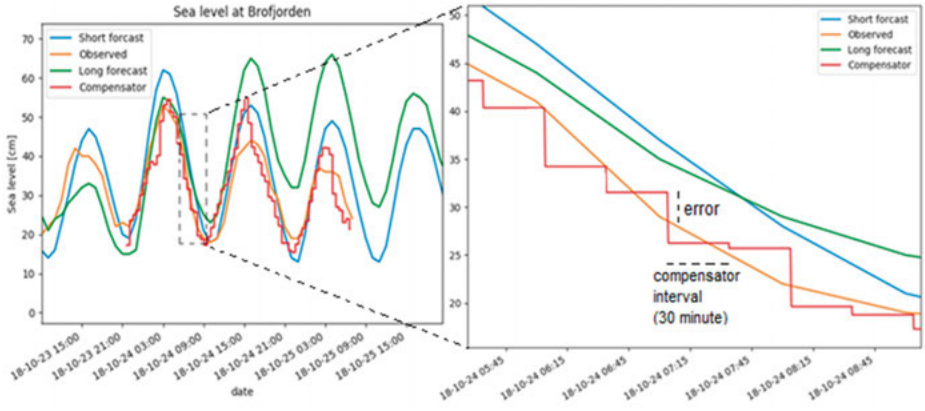

Figure 4.1. The result of the positioning test of the compensator. Right: Zoomed-out area marked by a dashed rectangle (Figure 13 in Paper V).

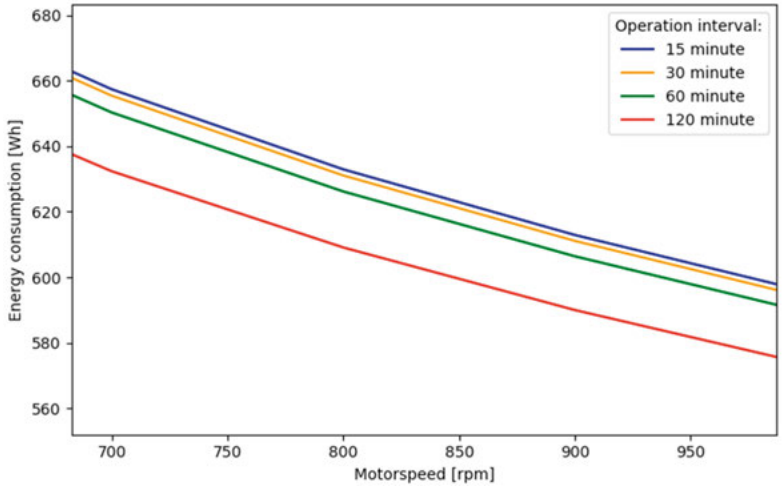

Figure 4.2. Estimated energy consumption for 24 hours with different adjustment time intervals and motor speeds for operation in Wave Hub (Figure 16 in Paper V).

Table 4.2. Root mean square error (RMSE) of the compensator position relative to the actual sea level for different control strategies at Wave Hub.

Interval time [minutes]	**RMSE [cm]**
15	17
30	34
60	67
120	130

From the analysis of the speed control and the adjustment time interval, a conclusion can be drawn that the effect of the adjustment time interval on the power consumption is minimal (see Fig. 4.2). However, the longer the adjustment time interval, the larger the error between the position of the compensator and the actual sea level (shown as *error* in Figure 4.1, RMSE in Table 4.2).

With reference to [52] and [53], the negative effects of the error in translator position on the power production are minimal when the tidal variation is in the range of 0.2 meters at the Wave Hub. As can be inferred from Table 4.2, a time interval of 15 minutes (or shorter) can keep the error of the compensator position compared to the sea level smaller than 0.2 meters the whole time. Another important finding is that the daily standby energy is around 125 Wh, which is significant for the case of Brofjorden where the total energy consumption required is around 170 Wh (Paper V). The standby energy is less dominant in the case of Wave Hub where the total energy consumption is around 600 to 640 Wh. As the batteries for the system are rated at 100 Ah, 24V, the energy should last for 3 days without recharging.

4.2. Wave energy potential in the Nordic countries

The ability of the WECs and wave farms to convert wave energy into electric energy was assumed to be 25% based on a number of previous studies [23], [54]–[57]. Table 4.3 shows the resulting distribution, by country, of wave power parks for the energy scenarios of 1, 3, 10 and 50 TWh yearly.

Table 4.3. The geographical distribution of the WEC's installed capacity as a result of the weighted and randomized allocation model. The regions studied include the east of Denmark (DK2), Finland (FI), Norway (NO), and Sweden (SE). The values are expressed in megawatt (MW).

	1 TWh	**3 TWh**	**10 TWh**	**50 TWh**
DK2	0	1.68	5.32	49.75
FI	1.97	4.94	8.93	42.29
NO	330	1000	3338	16728
SE	5.29	17.44	63.49	267.82
No. of wave farms	**60**	**177**	**584**	**2903**

Within the studied region, Norway has the highest potential for energy production compared to the other countries. The reason for this is the fact that Norway has a long coast and with an average energy flux intensity which is much higher than the other Nordic countries. Fig. 4.3 shows the distribution of wave farms for different scenarios. The color and the size of the dots indicate the installed power and the relative size of the wave farm, respectively. It should be noted that the size of the dots are not in scale, resulting in a more crowded appearance than in reality. They have been scaled up for better visibility.

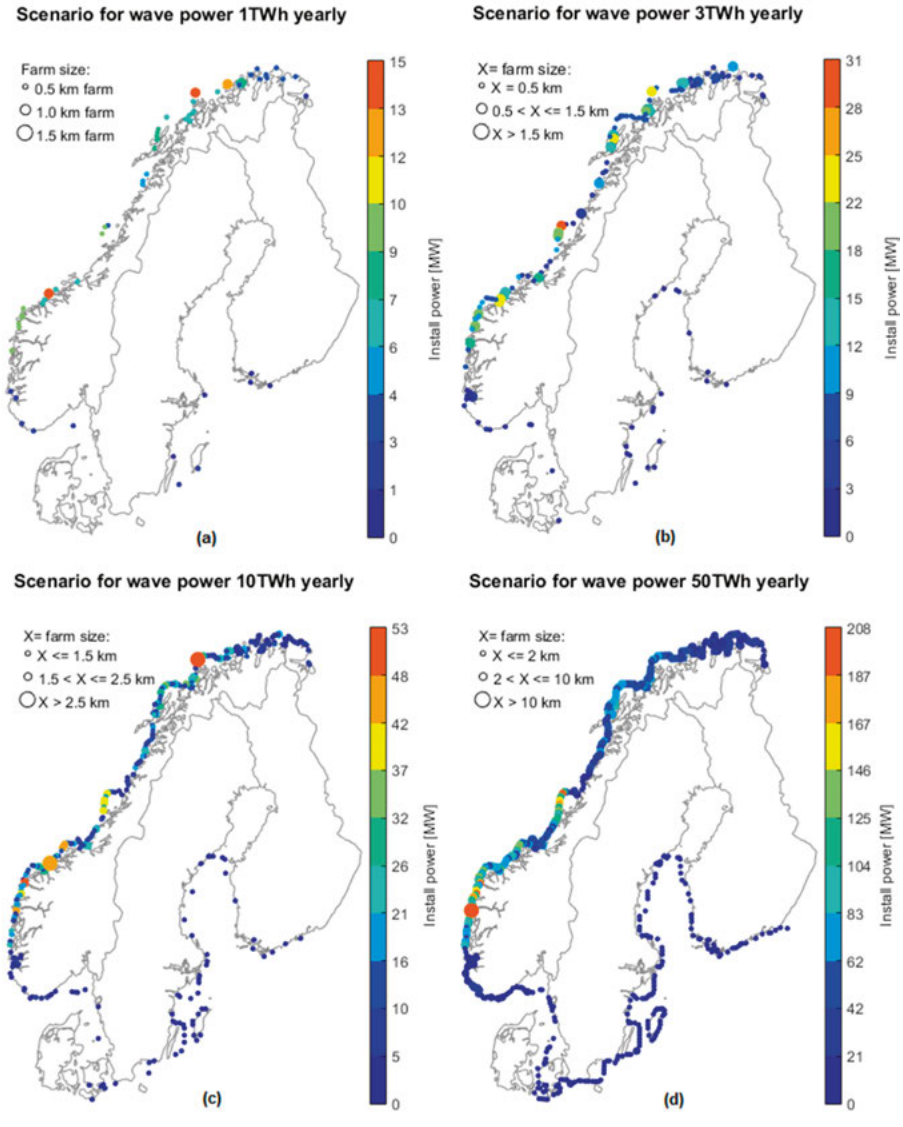

Figure 4.3. A stochastic distribution of wave farms for four energy scenarios. (a) 1 TWh scenario. (b) 3 TWh scenario. (c) 10 TWh scenario. (d) 50 TWh scenario (Figure 3 in Paper VI).

4.3. Net load variability in the Nordic countries

Fig. 4.4 shows the normalized standard deviation for the four frequency components (short-, mid-, mid/short-, and long-term components) in the 3 TWh scenario. In general, σ_{raw} varies between the IRE sources. In terms of fre-

quency components, the IRE sources clearly have different dominating frequency bands. For the short-term component, PV has the highest standard deviation, which is 80% of the σ_{raw}. Wave energy has a significant dominating variability for the long-term component, accounting for 48% of σ_{raw}. Wind and tidal energy have the most prominent variability for the mid- and mid/short-term components, which are 47% and 54% of σ_{raw}, respectively. The case for PV can be used to better understand the meaning of these results. For PV the σ_{raw} is equal to 1.76. This relatively high number is due to significantly high variations of PV power production in the Short-term frequency band (periods shorter than 2 days). A high variation in this frequency band is natural since it includes the difference in solar irradiations between day and night. Furthermore, the variation of PV is also high in the Long-term frequency band. This is also natural as it reflects the seasonal variations of solar irradiations in the Nordic countries – with a large difference between summer and winter. The high value of σ_{raw} for PV compared to the other IREs indicates that PV can be considered to be the most highly varying of the IRE sources studied.

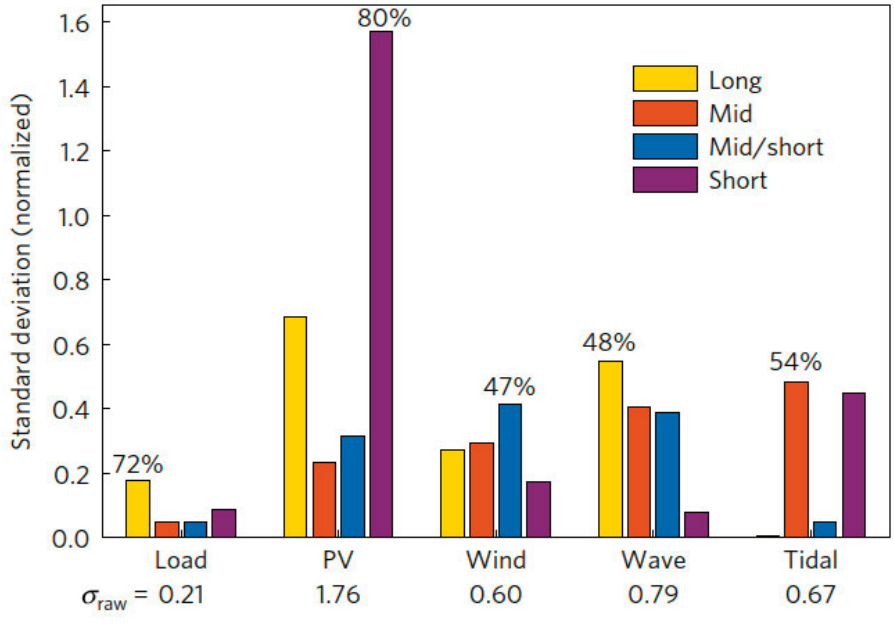

Figure 4.4. Standard deviations (normalized to the mean power generation) for load and IRE (PV, wind, wave, and tidal) generated based on four different timescales (Figure 2 in Paper VII).

Fig. 4.5 shows the result of the study on net load variability. The highly renewable and fully renewable scenarios are achieved with different mixes of IREs and the resulting variability is compared to variability of today. From

the figure, it is interesting to note that for σ_{LT}, σ_{ST}, and $\sigma_{\Delta P}$, mixes of IREs can be found so that the variability of the highly or fully renewable scenarios are not very different from today's variability. However, for σ_{MT} and σ_{MST} the variability was significantly higher regardless of the combination of IREs in the mix.

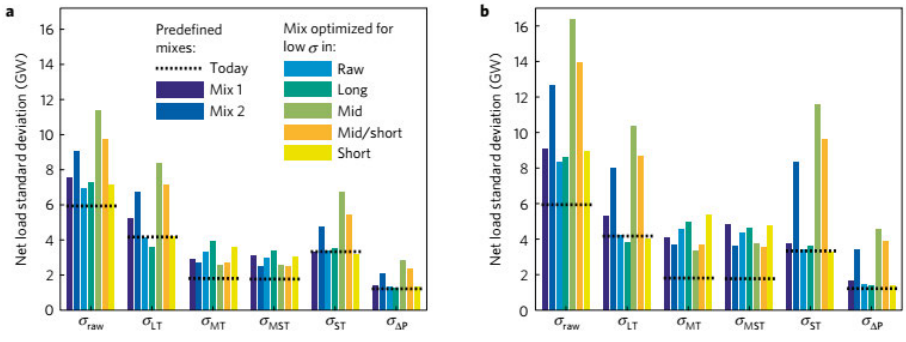

Figure 4.5. Net load standard deviation for different mixes compared to the present situation. (a) Highly renewable with 20% IREs (b) Fully renewable with 36% IREs. (Figure 4 in Paper VII)

5. Conclusions

The studies in the first part of the thesis evaluated the compensator both with simulations and experiments. The experiments were carried out in the lab at Uppsala University. To lift the actual 10 tonnes load with the setup in the lab environment would have posed a safety risk. Instead, the device compressed two stacks of springs up to a maximum load of 35 kN. The compensator system was characterized by the information gained in static- and dynamic-load tests. From these tests, the behavior of the system for different loads and different tides, as well as the power consumption, were calculated. For high tides it was shown that the operation time interval does not significantly affect the power consumption, but the error of the translator position in the linear generator will increase when a larger time interval is used.

Power production by a hybrid system consisting of solar PV and a small WEC to charge the battery of the compensator is necessary since there is no external power supply to the WEC's buoy. The small WEC and the solar panel complement each other; whereas the power production from solar PV will peak in summer, while the small WEC will peak during the winter.

The second part of the thesis addressed the question of how much wave energy is available to the Nordic synchronous grid. This study was then extended to include the possibilities for a highly or fully renewable power system in the Nordic synchronous grid.

The wave energy scenarios in the Nordic region was targeted to 1, 3, 10, and 50 TWh per year, corresponding to installed capacities of 337 MW, 1.02 GW, 3.42 GW, and 17.09 GW, respectively. The average annual wave energy resource for the Nordic synchronous grid is 570 TWh/year. All four IRE sources studied have shown a distinct variability pattern for different frequency bands. Due to strong seasonality and the diurnal pattern, PV is considered the most variable source. An optimized mix for low variability in any of σ_{raw}, σ_{LT}, σ_{ST}, and $\sigma_{\Delta P}$ will result in low variability in the others. However, regardless of the mix, a relatively large increase in the variability of the intermediate frequencies is inevitable. Nonetheless, this study has shown that a fully renewable Nordic power system is possible from the variability perspective.

6. Future Work

Currently, the main part of the compensator has been completed, with the force and control system tested experimentally (in the lab) and in simulations. However, there are some major issues that must be completed before the device is ready for full operation at sea:

1. The power supply system is still in the developmental phase even though it has been evaluated theoretically. A completed power supply system needs to be attached to the compensator, and an experiment with the actual load is needed to compare the measurements and the simulation.
2. A suitable design for the buoy is needed for the proper mounting and installment of the small WEC and the compensator.
3. Offshore tests for different tidal ranges need to be conducted to evaluate the integration of the compensator with the main WEC and its contribution to the power production of the main WEC.
4. A study of the economic benefits by taking account all the costs involved in the development of the tidal compensator for mass production.

7. Summary of papers

PAPER I

Wave Energy Research at Uppsala University and The Lysekil Research Site, Sweden: A Status Update.

The paper provides a status update of UU's wave energy research until 2015. In the paper, summarized works from different research topics are presented.

The author help out with experimental works related to the substation.

Presented by Arvind Parwal at the *Proceeding of the 11th European Wave and Tidal Energy Conference, Nantes, France, 6-11 Sept., EWTEC2015.*

PAPER II

Tidal Effect Compensation System Design for High Range Sea Level Variation.

The paper presents the mechanical parts of the tidal compensator. The illustration of the assembly and the result from the simulation are briefly described in this paper.

The author wrote and presented the paper at the *Proceeding of the 11th European Wave and Tidal Energy Conference, Nantes, France, 6-11 Sept., EWTEC2015.*

PAPER III

Small-Scale Renewable Energy Converters for Battery Charging.

In this paper, the power production from the small renewable energy converters to power the compensator are presented.

The author contributed to performing the analysis of the solar PV, model the small WEC, and writing the article.

Published in *Journal of Marine Science and Engineering*, 6, 26, 2018.

PAPER IV

Control Strategy for a Tidal Compensation System for Wave Energy Converter Device.

The electrical and control system is proposed together with the experimental setup of the compensator in the lab environment.

The author contributed to the work by building the device and experimental setup, building the control unit, and writing the paper.

Presented by the author at the *Proceedings of the Twenty-eighth (2018) International Ocean and Polar Engineering Conference Sapporo, Japan, June 10-15, 2018.*

PAPER V

A remotely controlled sea level compensation system for wave energy converters.

This paper presents experimental tests of the compensator in a lab environment. The objective is to evaluate the control strategy and model the system for power estimation.

The author design and performed the experiment, modeled the motor and developed the control system.

Submitted to *Energies* in April 2019.

PAPER VI

Wave energy potential and 1-50 TWh scenarios for the Nordic synchronous grid.

A model developed to estimate the wave energy potential in the Nordic countries. The target for four different scenarios are set as the objective function, and the size of the wave farms for the particular scenario was estimated.

The author contributed to developing the model, performing the simulation, and writing the article.

Publish in *Renewable Energy*, 101, 462-466, 2017.

Paper VII

Net load variability in Nordic countries with a highly or fully renewable power system.

The net load variability from IRE: wind, solar, wave and tidal, is studied for Nordic countries. The study investigates the effect of different shares of IRE with the aim to minimize the net load, based on the standard deviation of the mix in different time scales.

The author was responsible for the part of wave resource: collecting and analyzing wave data.

Published in *Nature Energy*, 16175, 2016.

8. Svensk sammanfattning

Del ett av denna avhandling behandlar utvecklingen av en tidvattenkompensator. Det koncept för vågenergiomvandlare (WEC) som utvecklats vid Uppsala Universitet baserar sig på en punktabsorberande boj kopplad till en linjärgenerator placerad på havsbotten. Translatorn inuti generatorn är kopplad till bojen via en stålvajer, och oscillerar linjärt. Uteffekten från systemet är optimal när translatorns rörelse är centrerad i mitten på statorn.

Translatorns genomsnittsposition kan emellertid förändras med tiden, exempelvis på grund av tidvatten. Varje avvikelse från den optimala positionen resulterar i en minskad effektutmatning. Detta kan resultera i en begränsning av produktionen för en WEC som är placerad i ett område med stor variation av den genomsnittliga havsnivån. Translatorn kan i extrema fall fastna i toppen eller vila i botten på generatorn en signifikant del av dagen.

En lösning till detta problem är att utveckla en tidvattenkompensator, kapabel att justera längden på vajern som kopplar ihop bojen med translatorn. Då den typiska vikten på detta system är runt 10 ton, så bedömdes ett kedjehjul med stålkedja vara nödvändig. Det konstruerade kedjehjulet är vidare batteridrivet och fjärrstyrt, och behöver därför en pålitlig matning som laddar batterierna kontinuerligt.

Efter simulationer av två representativa vågklimat har en hybrid av solceller (PV) och en liten WEC föreslagits som primär källa för batteriladdningen. Detta för att systemet skall fungera året runt. Test i labbet har visat att tidvattenkompensatorn är kapabel att lyfta den uppskattade vikten på de rörliga delarna, samt att följa uppmätta variationer i genomsnittlig havsnivå orsakade av tidvatten.

Del två av denna avhandling består av en studie av potentialen för vågkraft i det nordiska elnätet. En modell för placering av vågfarmer, som baserar sig på fyra energiscenarier, har utvecklats och används för att hitta en optimal placering. Scenarierna baserar sig på total mängd implementerad vågkraft, från 1 TWh till 50 TWh årligen.

En vidareutveckling av denna studie behandlar en undersökning av den totala variabiliteten i elnätet (kombinationen av variabilitet i konsumtionen med den

i produktionen) för ett hypotetiskt nordiskt elnät helt baserat på förnybara energikällor. Det innefattade fyra typer av intermittenta förnybara energikällor: sol (PV), vind, tidvatten och vågor. Studien visar att en optimal kombination av dessa källor är kapabla att försörja det nordiska elnätet även i fallet med ett 100% förnybart kraftsystem.

Acknowledgments

First and foremost, I would like to say alhamdulillah; with His blessing I finish this last part of my thesis.

I would like to express my gratitude to the supervisor of my Ph.D. work, Prof. Rafael Waters, for giving me the opportunity to carry out this Ph.D., for always being positive and supportive, for being around to hear and respond to my enquiries and to show me the way to do things right, not to mention for giving me a chance to learn from my mistakes. It was a wonderful experience to be part of your team.

Thanks to Prof. Mats Leijon for giving me the opportunity to be part of the wave energy family at Uppsala University.

To my co-supervisor, Johan Abrahamsson – thank you for always being around for all the no-appointment consultations and for giving me technical advice on the project.

My utmost appreciation goes to the Ministry of Education in Malaysia and Universiti Malaysia Perlis for providing me with four years of financial support during my doctoral study in Sweden. I would like to extend this appreciation to Uppsala University for funding me during the remaining period of my study.

Special thanks to Valeria Castellucci for co-authoring my papers and for being actively involved in the compensator project. Thank you for the valuable time you spent helping me with the project and for the knowledge and experience you shared.

I would like to extend my sincere appreciation to Olle Svensson for all the technical advice and expertise you shared during the course teaching and the research.

Thank you, Ingrid, Lena and Per-R L., for taking care of the administrative issues related to the studies, and Thomas, for the speedy responses whenever I faced a problem with my machines.

Thanks to Muzaffar and Dalina for introducing me to Ph.D. life in Sweden, for all the good times we spent together, from coffee time in the lounge to berries time by the river Uppsala. To Khadijah, for having a glance at my thesis when I was halfway in writing it. To Arvind, for being an awesome colleague and neighbor – thanks for your advice and encouragement.

To my officemates, present and past: Anke, Per R., Simon, Erini, Kaspars, and Akif. I will not forget the wonderful time we spent together. Thank you for sharing a nice working place.

Special thanks to my friends at the Division of Electricity and Ångström Laboratoriet: Saman, Andre, Juan, Jose, Pasan, Irina, Flore, Minh Thao, Johan F., Tobias, Aya, Malin, Jens, Bahri, Victor, Tatiana, Maria, Jennifer, Ana, Liguo, Francesco, Brenda, and all who were on the Lysekil trips, and everyone else. It was a pleasure to know you.

To my Malaysian friends in Uppsala, present and past: Khadijah, Fadli & Siti, Shahar & Sikin, Syaiful, Ida, Ahmad Bijairimi & Yasmin, Akma, Wooi, Edison, and Lai Mun for the laughter, the gatherings, and, not to forget, the food!

Special thanks go to my beloved late father, my mother, my father- and mother-in-law, Kak and Abg Lan, Ina and Mat, Abg Lid, Kak Noraini, Kak Niza, Fakhrul and Zila, Ija and Khoiri, Aziyah and Anas, Adlina and Firdaus, and Jijah and Hazim – for the support and prayers and for being awesome!

Finally, to my beloved wife, Azhan, and my kids, Zakwan and Iman, for always being understanding and supportive, for always being by my side through this bumpy journey, and for always putting a smile on my face.

To all the people who have given me their support and help, directly or indirectly – I will always be grateful.

Nasir Ayob
Spring 2019, Uppsala

References

[1] REN21, REN21. Renewables 2018-global status report, Paris, REN21 Secretariate; 2018. 2018.

[2] L. Sjökvist, R. Krishna, M. Rahm, V. Castellucci, A. Hagnestål, and M. Leijon, "On the Optimization of Point Absorber Buoys," J. Mar. Sci. Eng., vol. 2, no. 2, pp. 477–492, May 2014.

[3] J. Engström, M. Eriksson, J. Isberg, and M. Leijon, "Wave energy converter with enhanced amplitude response at frequencies coinciding with Swedish west coast sea states by use of a supplementary submerged body," J. Appl. Phys., vol. 106, no. 6, p. 064512, Sep. 2009.

[4] J. Engström, V. Kurupath, J. Isberg, and M. Leijon, "A resonant two body system for a point absorbing wave energy converter with direct-driven linear generator," J. Appl. Phys., vol. 110, no. 12, p. 124904, Dec. 2011.

[5] L. Hai, O. Svensson, J. Isberg, and M. Leijon, "Modelling a point absorbing wave energy converter by the equivalent electric circuit theory: A feasibility study," J. Appl. Phys., vol. 117, no. 16, 2015.

[6] M. Giassi and M. Göteman, "Layout design of wave energy parks by a genetic algorithm," Ocean Eng., vol. 154, no. March 2017, pp. 252–261, 2018.

[7] A. F. d. O. Falcão, "Wave energy utilization: A review of the technologies," Renew. Sustain. Energy Rev., vol. 14, no. 3, pp. 899–918, 2010.

[8] B. Drew, a. . Plummer, and M. . Sahinkaya, "A review of wave energy converter technology," vol. 223, pp. 887–902, 2009.

[9] E. Wintz, "Wave Power Energy." [Online]. Available: https://wavepoweralternativeenergy.weebly.com/oscillating-water-column.html.

[10] M. Rahm, "Ocean Wave Energy : Underwater Substation System for Wave Energy Converters," Acta Universitatis Upsaliensis, Electricity, Department of Engineering Sciences, Technology, Disciplinary Domain of Science and Technology, Uppsala University, 2010.

[11] J. P. Kofoed, P. Frigaard, E. Friis-Madsen, and H. C. Sørensen, "Prototype testing of the wave energy converter wave dragon," Renew. Energy, vol. 31, no. 2, pp. 181–189, 2006.

[12] "Wave Dragon." [Online]. Available: http://www.wavedragon.co.uk.

[13] R. Waters, J. Engström, J. Isberg, and M. Leijon, "Wave climate off the Swedish west coast," Renew. Energy, vol. 34, pp. 1600–1606, 2009.

[14] M. Leijon, C. Boström, O. Danielsson, S. Gustafsson, K. Haikonen, O. Langhamer, E. Strömstedt, M. Stålberg, J. Sundberg, O. Svensson, S. Tyrberg, and R. Waters, "Wave energy from the north sea: Experiences from the lysekil research site," Surv. Geophys., vol. 29, pp. 221–240, 2008.

[15] R. Ekström and M. Leijon, "FPGA Control Implementation of a Grid-Connected Current-Controlled Voltage-Source Inverter," J. Control Sci. Eng., vol. 2013, pp. 1–10, 2013.

[16] A. Parwal, M. Fregelius, I. Temiz, M. Göteman, J. G. de Oliveira, C. Boström, and M. Leijon, "Energy management for a grid-connected wave energy park through a hybrid energy storage system," Appl. Energy, vol. 231, pp. 399–411, 2018.
[17] M. Stalberg, R. Waters, O. Danielsson, and M. Leijon, "Influence of Generator Damping on Peak Power and Variance of Power for a Direct Drive Wave Energy Converter," J. Offshore Mech. Arct. Eng., vol. 130, no. 3, pp. 1–4, 2008.
[18] R. Ekström, V. Kurupath, O. Svensson, and M. Leijon, "Measurement system design and implementation for grid-connected marine substation," Renew. Energy, vol. 55, pp. 338–346, 2013.
[19] "Deployment and Maintenance of Wave Energy Converters at the Lysekil Research Site: A Comparative Study on the Use of Divers and Remotely-Operated Vehicles," J. Mar. Sci. Eng., vol. 6, no. 2, p. 39, 2018.
[20] F. Remouit, "Automation of underwater operations on wave energy converters using remotely operated vehicles," Acta Universitatis Upsaliensis, Electricity, Department of Engineering Sciences, Technology, Disciplinary Domain of Science and Technology, Uppsala University, 2018.
[21] M. Göteman, J. Engström, M. Eriksson, and J. Isberg, "Fast modeling of large wave energy farms using interaction distance cut-off," Energies, vol. 8, no. 12, pp. 13741–13757, 2015.
[22] R. Ekström and M. Leijon, "Control of offshore marine substation for grid-connection of a wave power farm," Int. J. Mar. Energy, vol. 5, pp. 24–37, 2014.
[23] M. Göteman, J. Engström, M. Eriksson, and J. Isberg, "Optimizing wave energy parks with over 1000 interacting point-absorbers using an approximate analytical method," Int. J. Mar. Energy, vol. 10, pp. 113–126, Jun. 2015.
[24] A. Bender and J. Sundberg, "Effects of Wave Energy Generators on Nephrops norvegicus," in AWTEC 2018 Proceedings :, 2018.
[25] F. Francisco and J. Sundberg, "Detection of Visual Signatures of Marine Mammals and Fish within Marine Renewable Energy Farms using Multibeam Imaging Sonar," J. Mar. Sci. Eng., vol. 7, no. 2, p. 22, 2019.
[26] V. Castellucci, J. Abrahamsson, T. Kamf, and R. Waters, "Nearshore Tests of the Tidal Compensation System for Point-Absorbing Wave Energy Converters," Energies, vol. 8, no. 4, pp. 3272–3291, Apr. 2015.
[27] "European Centre for Medium-Range Weather Forecasts," 2015. [Online]. Available: http://apps.ecmwf.int/datasets/data/interim-full-daily. [Accessed: 18-Mar-2017].
[28] The Open University, "Chapter 2 - Tides," in Open University Oceanography, B. T.-W. The Open University Tides and Shallow-Water Processes, Ed. Oxford: Butterworth-Heinemann, 1999, pp. 50–86.
[29] "Tides explained." [Online]. Available: http://beltoforion.de/article.php?a=tides_explained&p=tidal_cycles. [Accessed: 21-Mar-2019].
[30] C. Cenedese and R. A. R. Tricker, "Wave," Encyclopædia Britannica, inc., 2018. [Online]. Available: https://www.britannica.com/science/wave-water. [Accessed: 23-Mar-2019].
[31] A. Pecher, J. P. Kofoed, M. Folley, R. Costello, J. H. Todalshaug, L. Bergdahl, A. Têtu, and M. Alves, Handbook of Ocean Wave Energy, vol. 7. Cham: Springer International Publishing, 2017.
[32] J. Falnes, "A review of wave-energy extraction," Mar. Struct., vol. 20, no. 4, pp. 185–201, 2007.

[33] K. Budal and J. Falnes, “Wave power conversion by point absorbers: A Norwegian project,” Int. J. Ambient Energy, vol. 3, no. 2, pp. 59–67, 1982.
[34] V. Castellucci, “Sea Level Compensation System for Wave Energy Converters,” Uppsala University, Electricity, 2016.
[35] J. J. Stoker, “Basic Hydrodynamics,” in Water Waves, Hoboken, NJ, USA: John Wiley & Sons, Inc., 2011, pp. 1–18.
[36] A. F. O. Falc??o and J. C. C. Henriques, “Oscillating-water-column wave energy converters and air turbines: A review,” Renew. Energy, vol. 85, pp. 1391–1424, 2016.
[37] A. J. Garrido, E. Otaola, I. Garrido, J. Lekube, F. J. Maseda, P. Liria, and J. Mader, “Mathematical Modeling of Oscillating Water Columns Wave-Structure Interaction in Ocean Energy Plants,” Math. Probl. Eng., vol. 2015, no. Figure 2, pp. 1–11, 2015.
[38] A. da Rosa, “Wind Energy,” in Fundamentals of Renewable Energy Processes, Elsevier, 2013, pp. 685–763.
[39] S. Thomas, M. Eriksson, M. Göteman, M. Hann, J. Isberg, and J. Engström, “Experimental and numerical collaborative latching control of wave energy converter arrays,” Energies, vol. 11, no. 11, 2018.
[40] L. Sjökvist, M. Göteman, M. Rahm, R. Waters, O. Svensson, E. Strömstedt, and M. Leijon, “Calculating buoy response for a wave energy converter—A comparison of two computational methods and experimental results,” Theor. Appl. Mech. Lett., vol. 7, no. 3, pp. 164–168, 2017.
[41] M. A. Chatzigiannakou, I. Dolguntseva, and M. Leijon, “Offshore Deployment of Point Absorbing Wave Energy Converters With a Direct Driven Linear Generator Power Take-Off at the Lysekil Test Site,” in Volume 9A: Ocean Renewable Energy, 2014, no. 45530, p. V09AT09A023.
[42] S. Tyrberg, O. Svensson, V. Kurupath, J. Engstrom, E. Stromstedt, and M. Leijon, “Wave Buoy and Translator Motions—On-Site Measurements and Simulations,” IEEE J. Ocean. Eng., vol. 36, no. 3, pp. 377–385, Jul. 2011.
[43] R. Waters, M. Stålberg, O. Danielsson, O. Svensson, S. Gustafsson, E. Strömstedt, M. Eriksson, J. Sundberg, and M. Leijon, “Experimental results from sea trials of an offshore wave energy system,” Appl. Phys. Lett., vol. 90, no. 3, p. 34105, Jan. 2007.
[44] E. Lejerskog, C. Boström, L. Hai, R. Waters, and M. Leijon, “Experimental results on power absorption from a wave energy converter at the Lysekil wave energy research site,” Renew. Energy, vol. 77, pp. 9–14, 2015.
[45] “British Oceanographic Data Centre.” [Online]. Available: https://www.bodc.ac.uk. [Accessed: 11-May-2016].
[46] M. Ayob, V. Castellucci, M. Göteman, J. Widén, J. Abrahamsson, J. Engström, and R. Waters, “Small-Scale Renewable Energy Converters for Battery Charging,” J. Mar. Sci. Eng., vol. 6, no. 1, p. 26, Mar. 2018.
[47] T. Huld, R. Müller, and A. Gambardella, “A new solar radiation database for estimating PV performance in Europe and Africa,” Sol. Energy, vol. 86, no. 6, pp. 1803–1815, Jun. 2012.
[48] “Swedish Meteorological and Hydrological Institute.” [Online]. Available: https://www.smhi.se. [Accessed: 08-Mar-2018].
[49] “CloudAMQP.” [Online]. Available: https://www.cloudamqp.com/.
[50] “ARDUINO MEGA 2560.” [Online]. Available: https://store.arduino.cc/arduino-mega-2560-rev3. [Accessed: 24-Jan-2018].

[51] M. N. Ayob, V. Castellucci, J. Abrahamsson, O. Svensson, and R. Waters, “Control strategy for a tidal compensation system for wave energy converter device,” in Proceedings of the International Offshore and Polar Engineering Conference, 2018, vol. 2018–June, pp. 808–812.
[52] V. Castellucci, M. Eriksson, and R. Waters, “Impact of Tidal Level Variations on Wave Energy Absorption at Wave Hub,” Energies, vol. 9, no. 10, p. 843, Oct. 2016.
[53] S. Tyrberg, R. Waters, and M. Leijon, “Wave power absorption as a function of water level and wave height: Theory and experiment,” IEEE J. Ocean. Eng., vol. 35, no. 3, pp. 558–564, 2010.
[54] J. Engström, M. Eriksson, M. Göteman, J. Isberg, and M. Leijon, “Performance of large arrays of point absorbing direct-driven wave energy converters,” J. Appl. Phys., vol. 114, no. 20, p. 204502, 2013.
[55] I. A. Ivanova, H. Bernhoff, O. Ågren, and M. Leijon, “Simulated generator for wave energy extraction in deep water,” Ocean Eng., vol. 32, no. 14–15, pp. 1664–1678, Oct. 2005.
[56] K. Thorburn, H. Bernhoff, and M. Leijon, “Wave energy transmission system concepts for linear generator arrays,” Ocean Eng., vol. 31, pp. 1339–1349, 2004.
[57] A. Babarit, J. Hals, M. J. Muliawan, A. Kurniawan, T. Moan, and J. Krokstad, “Numerical benchmarking study of a selection of wave energy converters,” Renew. Energy, vol. 41, pp. 44–63, 2012.

Acta Universitatis Upsaliensis

Digital Comprehensive Summaries of Uppsala Dissertations from the Faculty of Science and Technology 1795

Editor: The Dean of the Faculty of Science and Technology

A doctoral dissertation from the Faculty of Science and Technology, Uppsala University, is usually a summary of a number of papers. A few copies of the complete dissertation are kept at major Swedish research libraries, while the summary alone is distributed internationally through the series Digital Comprehensive Summaries of Uppsala Dissertations from the Faculty of Science and Technology. (Prior to January, 2005, the series was published under the title "Comprehensive Summaries of Uppsala Dissertations from the Faculty of Science and Technology".)

Distribution: publications.uu.se
urn:nbn:se:uu:diva-381169

ACTA
UNIVERSITATIS
UPSALIENSIS
UPPSALA
2019